Title

Cloning and expression of a human kinesin heavy chain gene: interaction of the COOH-terminal domain with cytoplasmic microtubules in transfected CV-1 cells

Journal

Journal of Cell Biology, 117(6)

ISSN

0021-9525

Authors

Navone, F
Niclas, J
Hom-Booher, N
et al.

Publication Date

1992-06-15

DOI

10.1083/jcb.117.6.1263

Peer reviewed

Cloning and Expression of a Human Kinesin Heavy Chain Gene: Interaction of the COOH-terminal Domain with Cytoplasmic Microtubules in Transfected CV-1 Cells

Francesca Navone,*‡ Joshua Niclas,* Nora Hom-Booher,* Lynne Sparks,* Harris D. Bernstein,* Gretchen McCaffrey,* and Ronald D. Vale*

*Departments of Pharmacology and Biochemistry, University of California, San Francisco, San Francisco, California 94143; and ‡C. N. R. Center of Cytopharmacology, Department of Medical Pharmacology, Milano, Italy

Abstract. To understand the interactions between the microtubule-based motor protein kinesin and intracellular components, we have expressed the kinesin heavy chain and its different domains in CV-1 monkey kidney epithelial cells and examined their distributions by immunofluorescence microscopy. For this study, we cloned and sequenced cDNAs encoding a kinesin heavy chain from a human placental library. The human kinesin heavy chain exhibits a high level of sequence identity to the previously cloned invertebrate kinesin heavy chains; homologies between the COOH-terminal domain of human and invertebrate kinesins and the nonmotor domain of the *Aspergillus* kinesin-like protein *bimC* were also found. The gene encoding the human kinesin heavy chain also contains a small upstream open reading frame in a G-C rich 5′ untranslated region, features that are associated with translational regulation in certain mRNAs. After transient expression in CV-1 cells, the kinesin heavy chain showed both a diffuse distribution and a filamentous staining pattern that coaligned with microtubules but not vimentin intermediate filaments. Altering the number and distribution of microtubules with taxol or nocodazole produced corresponding changes in the localization of the expressed kinesin heavy chain. The expressed NH_2-terminal motor and the COOH-terminal tail domains, but not the α-helical coiled coil rod domain, also colocalized with microtubules. The finding that both the kinesin motor and tail domains can interact with cytoplasmic microtubules raises the possibility that kinesin could crossbridge and induce sliding between microtubules under certain circumstances.

KINESIN, a plus end–directed microtubule motor protein (Vale, 1987), has been characterized extensively using biochemical and molecular biological techniques. Mammalian kinesin is composed of two identical heavy chains (110–120 kD) and two identical light chains (60–70 kD) (Kuznetsov et al., 1988; Bloom et al., 1988) which together form an elongated structure with globular domains at either end (Amos, 1987; Hirokawa et al., 1989; Scholey et al., 1989). The heavy chain can be subdivided into three domains: a globular NH_2-terminal domain, a long rod domain, and a globular COOH-terminal tail domain (Yang et al., 1989; Kosik et al., 1990). The NH_2 terminal domain, which contains a consensus sequence for nucleotide binding (Yang et al., 1989), has been shown to generate microtubule movement in vitro (Yang et al., 1990) and has microtubule-stimulated ATPase activity (Kuznetsov et al., 1989); this region of kinesin is hence referred to as the motor domain. The middle of the kinesin heavy chain (KHC)[1] folds into a long α-helical coiled coil (rod domain) that enables the two heavy chains to dimerize (de Cuevas et al., 1992). The COOH-terminal globular tail domain interacts with the light chains (Hirokawa et al., 1989) and possibly other cytoplasmic components. Domains homologous to the kinesin motor have been found in a variety of other proteins, which are thought to be members of a large superfamily of microtubule-based motors (Vale and Goldstein, 1990; Endow, 1991; Goldstein, 1991). (In this paper, we shall refer to homologues as kinesin-like motors and refer to the originally described motor simply as kinesin).

Based upon in vitro observations that kinesin transports latex beads to the plus ends of microtubules (Vale et al., 1985), it was proposed that kinesin powers anterograde transport of organelles. Several recent experimental findings support this hypothesis. First, light and electron immunolocalization studies indicate that at least some of the kinesin is associated with membrane-bounded vesicles (Pfister et al., 1989; Hollenbeck, 1989; Wright et al., 1991; Hirokawa et al., 1991). Second, antikinesin antibodies cause the centripetal collapse of tubular lysosomes in macrophages (Hollenbeck and Swanson, 1990), inhibit pigment granule dispersion when microinjected into melanophores (Rodionov et al.,

1. *Abbreviations used in this paper*: hKHC, human kinesin heavy chain; KHC, kinesin heavy chain; ORF, open reading frame; PCR, polymerase chain reaction; VSV, vesicular stomatitis virus.

1991), and inhibit organelle transport when added to squid axoplasm (Brady et al., 1990). Finally, inhibition of kinesin expression in hippocampal neurons by antisense oligonucleotides (Ferreira et al., 1992) and the creation of mutations in the *Drosophila* kinesin gene (Saxton et al., 1991) both result in neuronal defects that are consistent with impaired axonal transport. In addition to transporting membrane vesicles, kinesin may have other biological functions. Kinesin, for example, was found to crossbridge and produce sliding between microtubules (Urrutia et al., 1991) and may transport intermediate filaments to the cell periphery (Gyoeva and Gelfand, 1991).

To understand the biological roles performed by kinesin, it is important to determine its interactions with subcellular structures and decipher how these interactions are regulated. In this study, we have isolated and sequenced a human cDNA encoding a gene that shows a high degree of amino acid sequence identity to the previously cloned invertebrate KHC genes (Yang et al., 1989; Kosik et al., 1990; Wright et al., 1991). Different domains of this KHC were expressed in CV-1 African green monkey kidney epithelial cells and their subcellular localizations determined. While the rod domain shows a predominantly soluble distribution, we find that the entire KHC, the motor domain, and the COOH-terminal tail domain all can interact with cytoplasmic microtubules.

Materials and Methods

Generation of Mammalian KHC Probe

The KHC nucleotide probe used for screening a human cDNA library was generated by the polymerase chain reaction (PCR) (Mullis et al., 1986). Specifically, MDCK cell first-strand cDNA was incubated with 500 pmol of a 128-fold degenerate 20 mer (5'-GA[GA]GA[GATC]ACCGT[GC]GC-[GATC]AA[GA]GA-3') and 18 mer (5'-[TC]TGCA[GA][GA]TC[TC]TG-[GATC]AC[GA]AA-3') (these two sequences were based upon amino acids 781–787 and 798–803 of the *Drosophila* KHC, respectively) in 67 mM Tris-HCl, pH 8.8, 6.7 mM $MgCl_2$, 16.6 mM ammonium sulfate, 10 mM 2-mercaptoethanol, 6.7 μM EDTA, 10% DMSO, 1.25 mM each of dNTP and 1 U Taq polymerase (Perkin-Elmer Cetus Instrs., Norwalk, CT) in a 50-μl reaction. Reactions were carried out for 50 cycles (93°C for 60 s, 48°C for 60 s, 55°C for 30 s) and then analyzed by PAGE. For sequencing of the PCR products, the reactions were run as above, but the degenerate 20 mer was endlabeled with ^{32}P (Maniatis et al., 1982). The radiolabeled PCR products were separated by PAGE as before, and a band of the expected size was excised from the gel. The radiolabeled fragment was extracted and then sequenced (Maxam and Gilbert, 1977) and found to encode a portion of a protein that was highly homologous to invertebrate KHCs.

cDNA Library Screening

A radioactive probe for library screening was prepared from the PCR-generated fragment. Specifically, 100 ng of the 20 mer and 18 mer, 5 U of the Klenow fragment of DNA polymerase I (Bethesda Research Laboratories, Gaithersburg, MD), 100 ng of the PCR fragment, 0.1 mM each of dGTP, dCTP, and dTTP, and 200 μCi of α[^{32}P]dATP (ICN Biomedicals, Inc., Costa Mesa, CA) were combined in 20 mM Tris-HCl, pH 7.5, 10 mM $MgCl_2$, 5 mM DTT, and incubated for 1 h at 23°C. This probe was then used to screen a human placental λgt11 cDNA library (generous gift from J. Evan Sadler, Washington University, St. Louis, MO) by plaque hybridization (Maniatis et al., 1982).

Sequence Analysis and Structure Prediction

Sequencing templates were generated by restriction fragment subcloning into M13 vectors or by making nested deletions with exonuclease III (Henikoff, 1987). Both strands of all clones were sequenced by the dideoxy chain termination technique (Sanger et al., 1977) using the USB Sequenase kit. Sequence analysis programs (Molecular Biology Information Resource, Department of Cell Biology, Baylor College of Medicine, Houston, TX) and structure prediction programs (Feiner-Moore and Stroud, 1984) were used as described. The computer search comparing different sequences of kinesin and kinesin-like proteins was performed using a Dayhoff scoring matrix (Lawrence and Goldman, 1988).

Construction of Vectors Expressing Human Kinesin Heavy Chain (hKHC)

Various portions of the human kinesin cDNA were synthesized using PCR; the full-length kinesin cDNA clone served as a template. The 5' PCR oligonucleotide in each reaction included an Xba site, the Kozak consensus sequence (Kozak, 1987), and the first 18 bases of the desired segment of the coding region. In the reactions for clones with an epitope tag, the 3' PCR oligonucleotide corresponded to the last 18 bases of the desired coding region, 39 bases encoding glycine and proline (as a flexible linker) and then vesicular stomatitis virus (VSV) G protein epitope tag (5'-CTTTCCAAG-ACGATTCATTTCGATGTCGGTGGGCCCCTGG-3'), a stop codon, and the SacI site. The 3' PCR oligonucleotide for the clones without an epitope tag included the last 18 bases of the desired coding region, a stop codon, and a BamHI site. The PCR reactions were done under the following conditions: 10 ng of cesium gradient–purified plasmid DNA was added to a mix containing 10 mM Tris, pH 8.3, 50 mM KCl, 2 mM $MgCl_2$, 0.01% gelatin, 0.2 mM dNTP, and 50 pmol of each oligonucleotide. The reactions were carried out at 94°C (60 s), 50°C (60 s), 72°C (3 min), for 30 cycles. The PCR products were subcloned into the SV-40 expression vector pSVL51 using either the XbaI, SacI, or BamHI sites (Huylebroeck et al., 1988).

Cell Culture

Unless otherwise indicated, CV-1 cells were grown in Dulbecco's minimum essential medium supplemented with 10% FCS, 4 mM L-glutamine, 100 U/ml penicillin, 100 μg/ml streptomycin, and 10 μg/ml gentamicin. Cells were maintained at 37°C under a 10% CO_2 atmosphere.

Transient Transfection of CV-1 Cells

20–24 h before DNA transfer, 70–80% confluent CV-1 cells were seeded 1:3 or 1:5 on acid-cleaned sterile glass coverslips. Transfections were performed following a DEAE–dextran precipitation method (Friederich et al., 1989; Huylebroeck et al., 1988). In all experiments, cesium chloride–purified plasmid DNA was dissolved to a final concentration of 20 μg/ml in minimum essential medium (with Earle's salts, 25 mM Hepes, L-glutamine) (MEM-Hepes, pH 7.15), without serum or sodium carbonate, but containing the same antibiotics as above. The DNA/MEM-Hepes solution was slowly added to an equal volume of 1 mg/ml DEAE-dextran (molecular mass 500,000; Pharmacia LKB Biotechnology Inc., Uppsala, Sweden) in MEM-Hepes (pH 7.25) and incubated for 30 min at room temperature after agitation. Cells were removed from the incubator, rinsed twice with MEM-Hepes, pH 7.25, and 100–150 μl of the DNA/DEAE-dextran mixture was added to each coverslip. After a 30-min incubation at room temperature, an excess of MEM-Hepes (pH 7.25) was added, the medium was removed, and cells were washed twice in the same medium. Supplemented Dulbecco's minimum essential medium containing 0.1 mM chloroquine diphosphate (Sigma Chem. Co., St. Louis, MO) was added, and cells were placed at 37°C for 3–4 h. The chloroquine treatment was followed by an overnight exposure of the cells to 0.1 mM sodium butyrate (Sigma Chem. Co.) in supplemented Dulbecco's minimum essential medium. Finally, cells were rinsed extensively with supplemented Dulbecco's minimum essential medium and grown for 24–48 h in the same medium before being analyzed. Proteins of the expected sizes were expressed in CV-1 cells from pSVTail, pSVRod, and pSVRT plasmids when examined by immunoblot analysis using a monoclonal antibody against the VSV G peptide.

Immunofluorescence Labeling

24–72 h after DNA transfer, cells were rinsed with PBS (140 mM NaCl, 2.7 mM KCl, 1.5 mM KH_2PO_4, 8.1 mM Na_2HPO_4, pH 7.2) and fixed by sequential immersions for 4 min each in methanol and acetone at −20°C. Cells were then immediately rehydrated in PBS before the staining reactions. When fixation was preceded by permeabilization, cells were treated in either one of the following ways: (*a*) after rinsing with PBS, coverslips were dipped four times for 25 s into four different breakers, each containing microtubule stabilizing buffer (80 mM Pipes-KOH, 1 mM EGTA, 1 mM $MgCl_2$, pH 6.8), 10% glycerol, and 0.5% Triton X-100 (modified from

Kreis [1986]); or (*b*) after rinsing with PBS, cells were incubated at 37°C for 10 min in 1% Triton X-100 in the same buffer as above (protocol modified from Hollenbeck [1989]). Both treatments produced similar results. Detergent treatment was then followed by methanol–acetone fixation. For immunofluorescence labeling, cells were processed through the following steps: (*a*) incubation with primary antibodies (see below) diluted in PBS (2 h); (*b*) wash with PBS (three to four times for 15 min); (*c*) incubation with affinity-purified Texas red–conjugated goat anti-rabbit IgGs and/or FITC-conjugated goat anti-mouse IgG (Axell Accurate Chemical Sci. Corp., Westbury, NY) (45 min; room temperature) (the rat monoclonals were efficiently recognized by the anti-mouse secondary IgGs); (*d*) washes with PBS (3–4 times for 15 min); and (*e*) a quick rinse in distilled water before mounting. Cells were observed using a photomicroscope III (Carl Zeiss, Inc., Thornwood, NY) equipped with epifluorescence, and photographs were taken using Tmax 400 film (Eastman Kodak Co., Rochester, NY).

The following primary antibodies were used in this study: (*a*) a polyclonal serum raised against squid KHC that was affinity purified against the bovine brain KHC by the method of Olmsted (1981); (*b*) monoclonal and affinity-purified polyclonal antibodies that recognize the COOH-terminal 10–amino acid epitope of the VSV G protein (Kreis, 1986), which were a kind gift from Drs. T. Kreis and R. Duden (EMBL, Heidelberg, Germany); (*c*) a rat antitubulin mAb (YL1/2) was a kind gift from Dr. J. Kilmartin (MRC, Cambridge, England), and; (*d*) a mAb against vimentin obtained from Boehringer Mannheim Corp. (Indianapolis, IN).

Quantitation of the Level of Kinesin Expression

The relative levels of kinesin expression were compared by quantitative video analysis. Cells containing the transiently expressed kinesin and/or endogenous kinesin were prepared for immunofluorescence as described above and reacted with the affinity-purified polyclonal antiserum against the squid KHC. The fluorescence signal was imaged with a Hamamatsu silicon-intensified target camera. The gain of the silicon-intensified target camera was first set so that the fluorescence signal from endogenous kinesin in the untransfected cells was within the linear range of the camera. At this gain, the fluorescence signal from the transfected cells generally saturated the camera. To bring the signal within the same linear range, neutral density filters were placed in the epifluorescence light path. The transmission characteristics of the filters were calibrated, so that signal could be normalized and the relative intensities from the transfected and nontransfected cells estimated. The images from the camera were stored digitally and analyzed using a Macintosh computer-based image analysis program (IMAGE - version 1.32; available from the National Technical Information Service, Springfield, VA). The average fluorescence intensities were measured for cells whose boundaries were marked manually.

SDS Gel Electrophoresis and Immunoblot Analysis

Proteins of total homogenates of CV-1 cells were separated on polyacrylamide gels under denaturing and reducing conditions (Laemmli, 1970) and immunoblotted (Towbin et al., 1979). Immunolabeling was performed using 5% nonfat dry milk, 10 mM Tris, pH 7.4, 150 mM NaCl, and 0.1% Tween-20 for all washes and incubations. Rabbit antibodies were detected by ^{125}I-conjugated protein A (Amersham Corp., Arlington Heights, IL) and autoradiography.

Results

Isolation of an hKCH cDNA

To obtain a hKHC cDNA, a nucleotide probe for screening cDNA libraries was first obtained by PCR. After comparing sequences of the *Drosophila* and squid KHC genes, two 128-fold degenerate pools of primers were synthesized based upon a highly conserved 35–amino acid sequence in the COOH-terminal domain (see Materials and Methods). With these primers, a unique fragment of the expected size (69 bp) was generated using first-strand cDNA derived from MDCK cells as a template. The sequence of this amplified DNA was ~75% identical at the nucleotide level and 100% identical at the amino acid level to the corresponding region of the squid (Kosik et al., 1990) or the *Drosophila* KHC genes (Yang et al., 1989), suggesting that the PCR product encoded a portion of a mammalian KHC gene.

The PCR-generated DNA fragment was used to screen a human placental λgt11 cDNA library. A 1.5-kb clone (λHK-3) obtained from the initial screen contained a large open reading frame that showed considerable homology to the COOH-terminal half of the squid and *Drosophila* KHCs and contained the sequence of the PCR fragment that was used as the probe. Rescreening of the library with a 5′ EcoRI–NcoI fragment of this partial clone produced a 3-kb clone (λHK-21), which contained the sequences of λHK-3 as well as an additional 1,250 nucleotides of coding sequence and 250 nucleotides in the 3′ untranslated region. Since λHK-21 did not encode a full-length KHC, a third screening using the 5′ NcoI–ApaLI fragment of λHK-21 was performed. This screen yielded a 1.4-kb clone (λHK-H8), which had a 700-nucleotide overlap with the 5′ end of λHK-21, the 5′ end of the coding sequence, and 313 nucleotides of the 5′ untranslated region. Another clone was later obtained that was identical to λHK-H8, except that it contained an additional 127 nucleotides at the 5′ end of the untranslated region. A hKHC cDNA (3.7 kb) containing the entire coding region as well as 313 bp of 5′ uncoding sequence and 482 bp of 3′ uncoding sequence (including an 82-base poly[A] tail) was created by joining λHK-H8 and λHK-21 together using a common PstI site.

Sequence Analysis and Comparison

The largest open reading frame (ORF) of the hKHC cDNA encodes a polypeptide of 963 amino acids (Fig. 1), which is similar in size to *Drosophila* (975 aa; Yang et al., 1989), squid (967 aa; Kosik et al., 1990), and sea urchin (1,031 aa; Wright et al., 1991) KHCs. The amino acid and nucleotide sequences are accessible through Genbank (accession number X65873). The amino acid sequence of hKHC displays a considerable identity throughout its length to the invertebrate KHCs (63% when compared with *Drosophila*) (Fig. 1). Even where amino acid sequences are different, many of the changes are conservative in nature. Secondary structure predictions using the method of Finer-Moore and Stroud (1984) also suggest that hKHC has an overall domain organization similar to that of previously described invertebrate KHCs (Yang et al., 1989; Kosik et al., 1990). Amino acids 1–413 of human kinesin (which contain a consensus sequence for ATP binding [aa 85–101]) are predicted to form a globular domain containing both α helices and β sheets. Adjacent to this putative motor domain is a long stretch of amino acids (aa 414–890; the rod domain) containing heptad repeats with hydrophobic amino acids prevalent in positions 1 and 4. The amphipathic nature of the helix is broken between residues 566 and 582 (the hinge region of the rod domain) and is weak between residues 460 and 470, 730 and 770, and 815 and 835. The COOH-terminal domain of hKHC (aa 890–963) is predicted to contain α helices, β sheets, and turns, which are suggestive of a more globular configuration. Based upon the high degree of primary and secondary structure similarities with invertebrate KHCs, we believe that our cloned cDNA encodes a human homologue of the KHC.

KHCs have not been found to share homology with a variety of kinesin-like proteins outside of their motor domains.

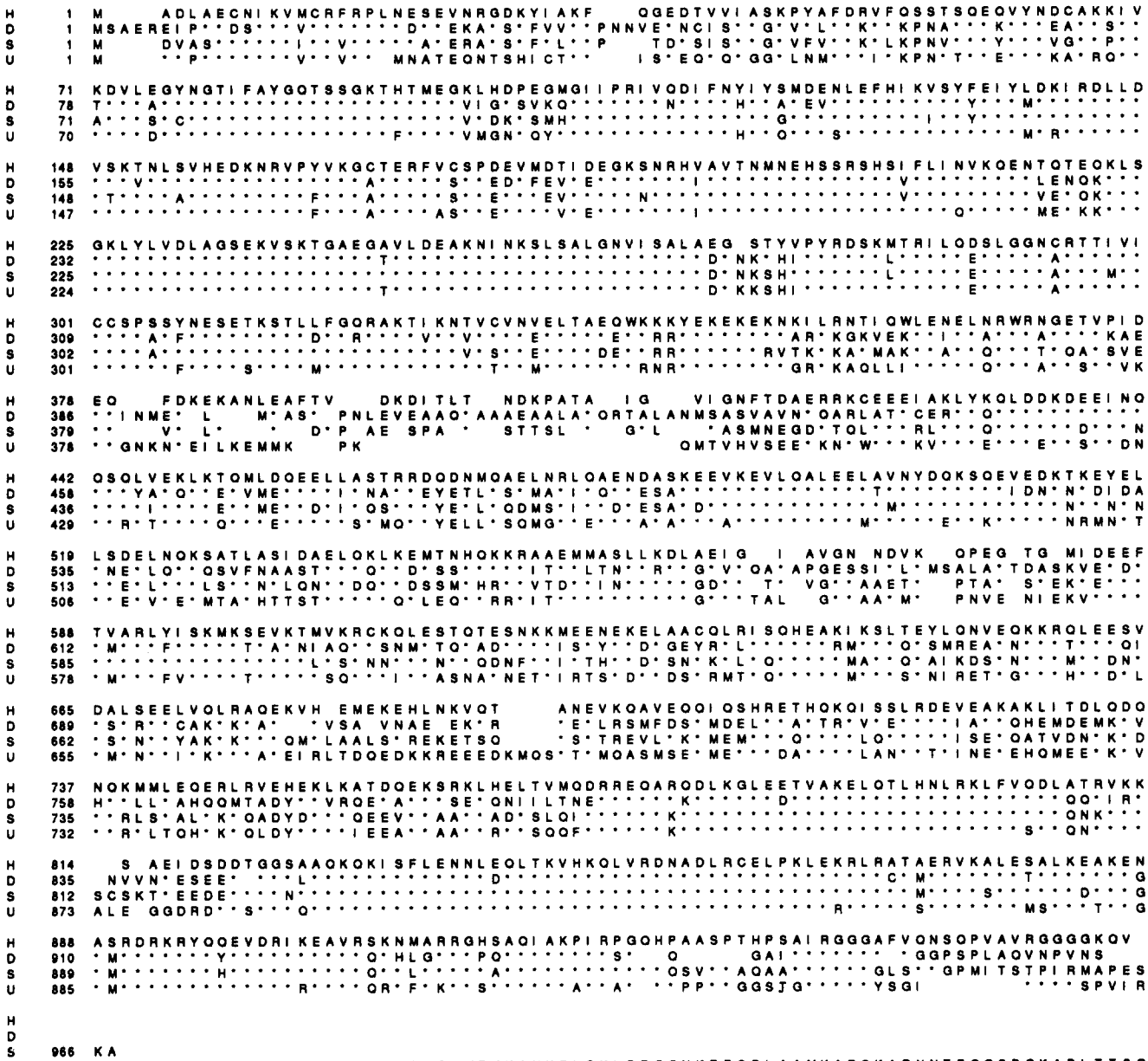

Figure 1. Alignment of the human and invertebrate KHC sequences. The three invertebrate KHCs—*Drosophila* (*D*), squid (*S*), and sea urchin (*U*)—were compared with the human (*H*) KHC sequence. Amino acids are numbered in the left margin. The one-letter amino acid code is used. Asterisks represent amino acid identities between a given invertebrate sequence and human. Blank spaces represent gaps that were introduced to maximize homology.

We reexplored this issue by aligning smaller segments of the hKHC with the kinesin-like genes *bimC* (Enos and Morris, 1990), KAR3 (Meluh and Rose, 1990), *cut7* (Hagan and Yanagida, 1990), *uncl04* (Otsuka et al., 1991), *ncd* (McDonald and Goldstein, 1990; Endow et al., 1990), and *nod* (Zhang et al., 1990). Our analyses revealed that *bimC* of *Aspergillus* (but none of the above kinesin-like proteins) contained segments of homology with the KHCs (Fig. 2). Two regions of similarity were noted. The first was a 14–amino acid stretch within the highly conserved end of the rod (aa 780–793 in human), which has seven identical residues, and three conservative changes in common with a region in the tail of *bimC* (aa 730–743). Another segment of 23 amino acids in the tail of KHC (aa 891–913 in human) also displayed significant homology to a region in the globular tail of *bimC* (aa 789–811). These findings suggest that the tail domains of *bimC* and the KHCs of higher eukaryotes have regions that may perform similar functions.

The 5′-untranslated region of hKHC has several features that are rarely found in eukaryotic mRNAs. This region, which is at least 440 nucleotides long, is longer than the 5′ untranslated regions found in most mammalian mRNAs (Kozak, 1987). It also contains unusually long stretches of G-C rich sequence (89.5% for nt −7 to −44, 75% for nt −53 to −96; 85.4% for nt −113 to −160; and 84.2% for nt −227 to −283) that may have the potential to form extensive secondary structure. The most unusual feature of the 5′-untranslated region, however, is the presence of three AUGs

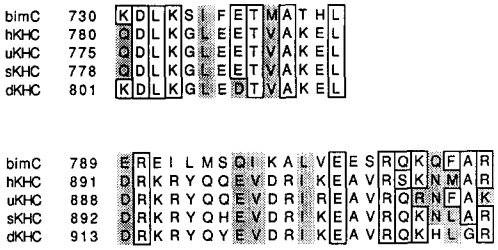

Figure 2. Nonmotor region comparison between the KHCs and the kinesin-like protein *bimC*. Comparison of the COOH-terminal domain of the human (*hKHC*), sea urchin (*uKHC*), squid (*sKHC*), and *Drosophila* (*dKHC*) KHCs to the nonmotor domains of *bimC* yielded these two regions of potentially meaningful homology. Amino acids are numbered in the left margin. Amino acid identity between *bimC* and any of the conventional KHCs is shown as a box. Shading indicates a conservative amino acid change. The SD scores for the upper and lower regions are 2.8 and 2.1, respectively, which indicates the number of SDs from that expected by a chance occurrence.

upstream from the KHC start codon (at nt −226, −217, and −214) followed by an in-frame termination codon at nt −203 (GCCGCCGCCATGGCTGCCATGATGGATCGGAAGTGA). This small open reading frame could encode a polypeptide of no more than eight amino acids. The first AUG of the upstream ORF is contained within a consensus initiation sequence (GCCGCCPuCCAUGG; [Kozak, 1987]).

Transient Expression of the hKHC Gene in CV-1 Cells

To study the interaction of different domains of the KHC with cytoplasmic structures, we expressed the hKHC gene or portions of the gene in CV-1 monkey kidney epithelial cells and examined the localization of the expressed proteins by immunofluorescence microscopy. Constructs containing the hKHC gene were prepared in the pSVL51 vector, which drives expression from a late SV-40 promoter and which replicates in CV-1 cells by virtue of expressing the SV-40 large T antigen. Constructs containing the following portions of the hKHC gene were used in this study: (*a*) the entire coding region of hKHC (pSVKin; aa 1–963), (*b*) the motor domain (pSVMot; aa 1–426), (*c*) a portion of the α-helical rod domain (pSVRod; aa 511–766), (*d*) the strongly conserved COOH-terminal portion of the α-helical coiled coil rod and the tail domain (pSVTail; 767–963), and (*e*) the COOH-terminal half of the protein containing the majority of the rod and the entire tail domain (pSVRT; 511–963). To localize the expressed protein unambiguously, nucleotides encoding the last 10 amino acids of the VSV G protein followed by a termination codon were added to the 3′ end of the above constructs. Monoclonal and polyclonal antibodies that recognize this peptide specifically (Kreis, 1986) were used to determine the location of the expressed protein by immunofluorescence.

Before examining the localization of the expressed hKHC, the distribution of the endogenous kinesin protein in CV-1 cells was determined using an affinity-purified polyclonal anti-KHC serum (originally prepared against SDS–polyacrylamide gel denatured squid KHC). By immunoblot analysis, the affinity-purified polyclonal antibody recognized a single 120-kD polypeptide in CV-1 crude extracts, which is

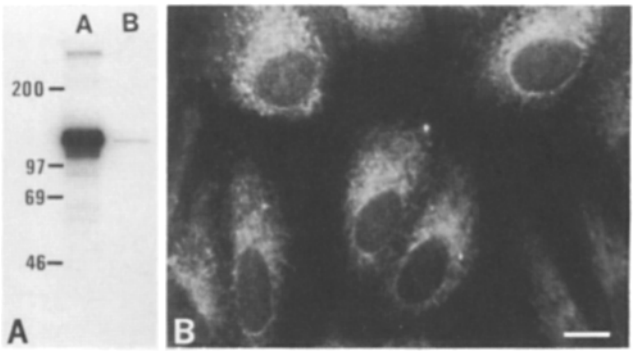

Figure 3. Immunofluorescence distribution of endogenous kinesin in nontransfected CV-1 cells (*A*) An immunoblot showing that an anti-KHC polyclonal antibody recognizes a unique band in a total homogenate of CV-1 cells (lane *B*; loading of 40 μg protein) which comigrates with purified bovine brain kinesin (lane *A*; loading of 1.5 μg protein). The migration of molecular weight standards are noted at the left. (*B*) Localization of endogenous kinesin in CV-1 cells as demonstrated by indirect immunofluorescence, using the same polyclonal serum as in *A*. CV-1 cells were grown to subconfluence on glass coverslips and fixed by methanol–acetone at −20°C. Bar, 1 μm.

the size expected for the KHC (Fig. 3 *A*). At a threefold greater protein loading, a very faint 45-kD band was also detected (not shown), which is the same size as a common proteolytic fragment of kinesin (Kuznetzov et al., 1989; Scholey et al., 1989). Immunofluorescence staining with the polyclonal antibody after methanol–acetone fixation revealed a diffuse distribution with some reticular features; neither filamentous nor vesicular staining was detected (Fig. 3 *B*). The faint reticular staining was retained after treatment with saponin (0.02%), but was substantially reduced by Triton X-100 (0.5%) permeabilization before fixation (not shown). This distribution of kinesin in nonextracted cells is similar to that reported by Hollenbeck (1989) in chicken embryo fibroblasts.

When CV-1 cells were transfected with pSVKin and fixed by methanol-acetone 24 h later, a strong immunofluorescence signal with the anti-VSV G peptide antibody was detected in ~10% of the cells, which are the ones believed to have been transfected with the plasmid (Fig. 4). The fluorescent signal from the remainder of the cells was extremely faint and only slightly greater than that produced by secondary antibody alone. This same weak staining is seen in cells that did not undergo the transfection procedure and thus probably represent untransfected cells in the population.

The distribution of hKHC expressed from pSVKin was somewhat different from that described above for the endogenous protein. A large amount of the expressed heavy chain was diffusely distributed throughout the cytoplasm; however, a filamentous pattern superimposed upon this diffuse staining was visible in most cells (Fig. 4 *A*). Filaments were not obvious in some cells, perhaps because of their prominent background staining. Filamentous patterns were also observed when the kinesin COOH-terminal tail (pSVTail) was expressed in CV-1 cells (Fig. 4 *C*). The filamentous patterns of the expressed KHC and the KHC tail domain coaligned with microtubules in these cells (Fig. 4, *B* and *D*). On the other hand, the kinesin rod domain (pSVRod) and the motor domain (pSVMot) displayed only a diffuse staining

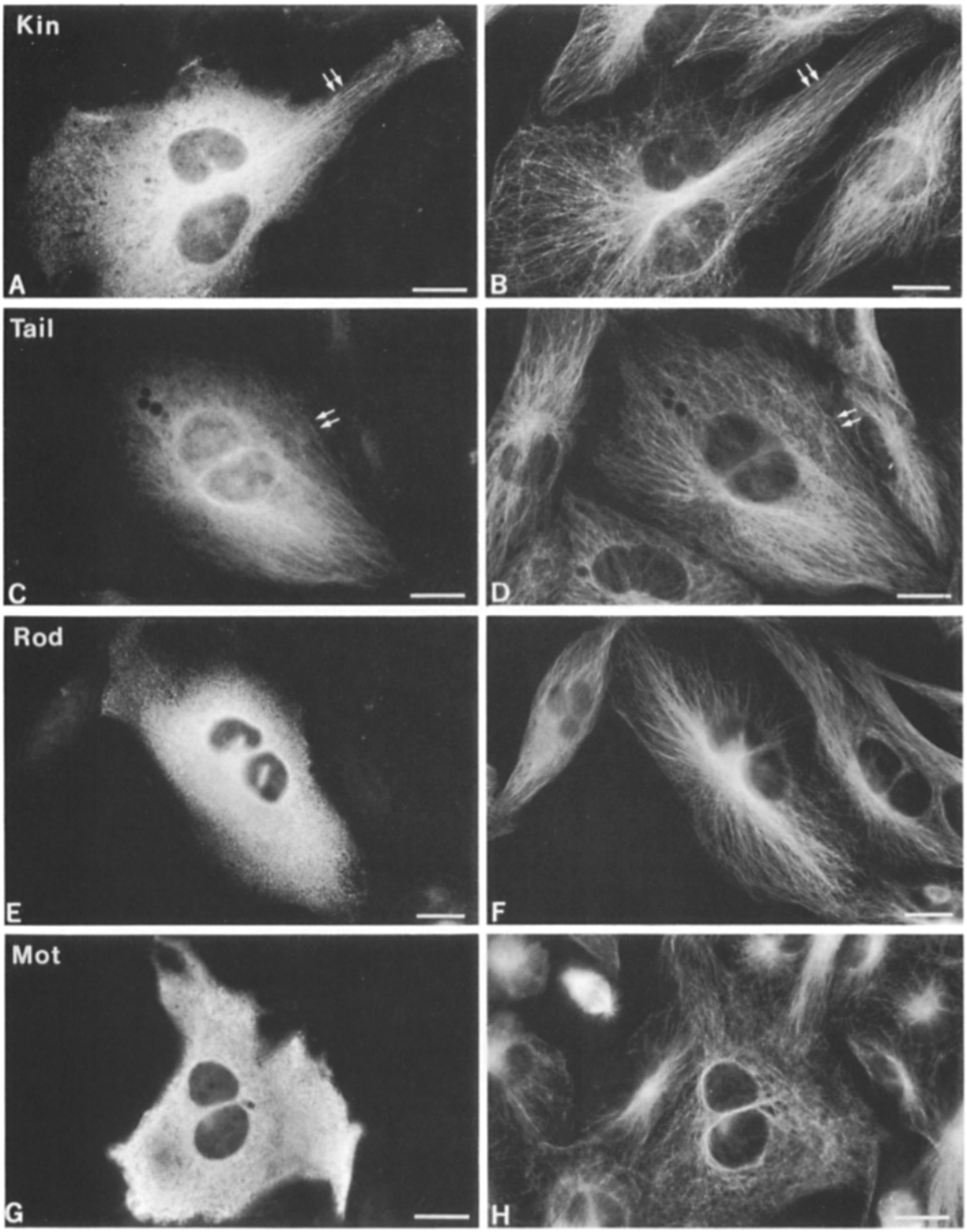

Figure 4. Indirect immunofluorescence of CV-1 cells expressing the entire KHC or portions of the KHC. Cells were transfected with the following constructs: (*A* and *B*) pSVKin; (*C* and *D*) pSVTail; (*E* and *F*) pSVRod; (*G* and *H*) pSVMot. All cells were fixed 24 h after transfection in methanol–acetone at −20°C. Cells were then double-labeled for the expressed kinesin proteins with rabbit polyclonal IgG against the VSV G peptide epitope (*C*, *E*, and *G*) and for tubulin with a monoclonal rat IgG (*B*, *D*, *F*, and *H*). In *A*, the expressed kinesin was visualized with the antikinesin polyclonal antibody; similar results were obtained with this construct with the anti-VSV G peptide polyclonal antibody. While the antitubulin antibody labels microtubules in all cells, the anti-VSV G peptide or antikinesin antibody produces an intense staining only in the transfected cells. In cells transfected with pSVKin (*A*) and pSVTail (*C*), the expressed kinesin proteins show a diffuse or faintly reticular distribution throughout the cytoplasm; superimposed on this pattern, filamentous staining is also evident (*A* and *C*, *arrows*) which coincides with microtubules (*B* and *D*, *arrows*). In cells transfected with pSVRod (*E*) and pSVMot (*G*), the expressed proteins are distributed throughout the cytoplasm and, in both cases, filamentous patterns were not observed. A greater percentage of transfected cells had multiple nuclei than untransfected cells, as shown in this figure. Multinucleate and uninucleate transfected cells, however, showed similar distributions of the expressed kinesin proteins. Bars, 2 μm.

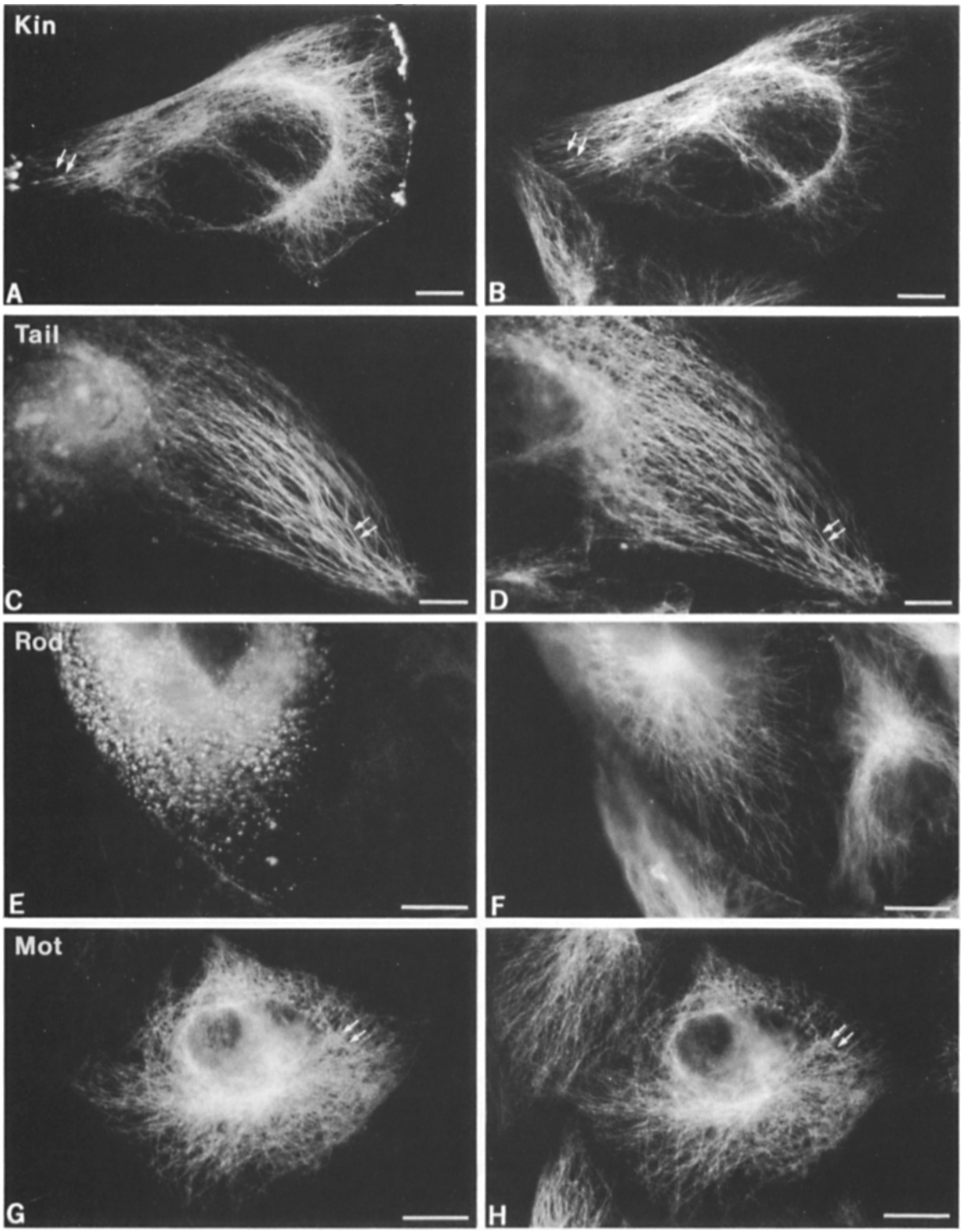

Figure 5. Indirect immunofluorescence micrographs illustrating the distribution of expressed kinesin proteins in CV-1 cells after detergent permeabilization. Cells were transfected with the following constructs: (*A* and *B*) pSVKin; (*C* and *D*) pSVTail; (*E* and *F*) pSVRod; (*G* and *H*) pSVMot. Cells were permeabilized with either 0.5% or 1% Triton X-100 in 80 mM Pipes, 1 mM EGTA, and 1 mM $MgCl_2$ before fixation in methanol–acetone at −20°C. Cells were then double-labeled for the expressed kinesin proteins with the polyclonal anti-G protein epitope antibody (*A*, *C*, *E*, and *G*) and for tubulin with the rat monoclonal (*B*, *D*, *F*, and *H*). In cells transfected with pSVKin (*A*) and pSVTail (*C*), treatment with Triton X-100 before the methanol–acetone fixation greatly reduces the diffuse and reticular staining of the cytoplasm which was evident in Fig. 7 (compare Fig. 7, *A* and *C*, with Fig. 8, *A* and *C*). The filamentous staining pattern for pSVKin, pSVTail, and pSVMot expressed proteins and the coalignment with microtubules is clearly evident (*A–D*, *G*, and *H*, *arrows*). In cells transfected with pSVRod that were Triton X-100 permeabilized before fixation, very few cells were found that displayed a strong immunofluorescence staining, probably because the soluble protein was removed by detergent treatment. The few cells that had a prominent immunofluorescence signal displayed an aggregated but not a filamentous staining pattern (*E*). The fine particulate immunofluorescence in *E* is probably due to artefactual precipitation of the expressed protein. Bars, 2 μm.

pattern (Fig. 4, *E* and *G*), as did the cytoplasmic bacterial enzyme β-galactosidase when expressed in CV-1 cells (not shown).

The localization of the expressed protein from pSVKin and pSVTail to filamentous cytoplasmic elements was clear in virtually all cells when soluble and membrane proteins were first extracted with Triton X-100 before fixation with methanol-acetone (Fig. 5, *A* and *C*). Saponin permeabilization and glutaraldehyde fixation produced identical results (not shown). The coalignment of these filamentous elements with microtubules also became more apparent after permeabilization (Fig. 5, *B* and *D*). The endogenous kinesin in untransfected cells did not show this filamentous distribution when fixed using a similar protocol. Such filamentous staining was also not observed with the expressed protein from pSVRod; in fact, very few immunoreactive cells could be detected, probably because the rod was soluble and hence washed away by the detergent treatment. In the few cells where immunoreactivity was detected, an aggregated but not a filamentous pattern was observed (Fig. 5, *E* and *F*). A small percentage (10%) of transfected cells exhibited large punctate staining suggestive of aggregated protein, regardless of the construct used or the fixation conditions.

After Triton X-100 permeabilization, the expressed motor domain demonstrated a filamentous staining that colocalized with microtubules (Fig. 5, *G* and *H*). This filamentous pattern, however, was not detected when 5 mM MgATP was included in the Triton X-100 permeabilization buffer; in this case, extremely few immunoreactive cells were observed, presumably because the motor domain was soluble and was washed away (not shown). Such ATP-dependent binding of the motor domain to cytoplasmic microtubules is consistent with biochemical experiments demonstrating that the motor domain exhibits a high affinity for microtubules only in the absence of ATP (Yang et al., 1989; Kuznetsov et al., 1989). The cellular concentrations of ATP probably account for why the motor domain does not localize to microtubules after direct methanol–acetone fixation (Fig. 4 *G*). Inclusion of 5 mM MgATP in the permeabilization buffer did not affect the colocalization of the tail domain with microtubules.

To be certain that the 10–amino acid VSV G protein epitope tag did not influence the distribution of the expressed proteins, the pSVKin and pSVRT constructs were prepared without the epitope tag and the expressed proteins were localized with the affinity-purified anti-KHC polyclonal antibody. The immunofluorescence signal obtained from the transfected cells was significantly greater than that of cells expressing only the endogenous kinesin, and thus the distribution of the expressed protein could be easily established. The immunofluorescence pattern observed for the expressed proteins without the epitope tag was indistinguishable from those shown in Figs. 4 and 5 (data not shown). Thus, we conclude that the 10 amino acids of the vesicular stomatitis virus G protein do not influence the distribution of the expressed kinesin proteins.

We also examined whether the level of KHC expression affected its distribution. pSVKin-expressed protein was compared to the endogenous KHC by performing immunofluorescence with the kinesin polyclonal antibody, imaging the cells with a video camera, and analyzing the relative intensities of stored digital images of cells using a computer program (see Materials and Methods). The majority of the cells (90%) had a low and fairly similar fluorescence signal attributable to the endogenous kinesin in the untransfected cells (100 cells analyzed). The transfected cells (10% of the population) had a much greater fluorescence signal; the fluorescence signal from 26% of the transfected cells was between 4- and 10-fold greater than that of untransfected cells, the signal from 47.3% of cells was 10–100-fold greater, and the signal from 26.7% of the cells was 100–500-fold greater (116 cells analyzed in total). All transfected cells exhibited both a cytoplasmic and a filamentous distribution of the expressed kinesin, regardless of the level of expression. In general, the cells expressing low levels of kinesin (four- to sixfold greater than endogenous kinesin) showed less numerous and more dimly stained filaments compared with high expressing cells, but these filaments were still always superimposable with microtubules. Thus, colocalization of the expressed KHC with microtubules was observed over a wide range of expression levels.

The transfected cells were generally larger (an average of 2.9-fold greater surface area) and more frequently binucleate than the untransfected cells. However, many of the transfected cells were small and contained only one nucleus; neither the size nor number of nuclei in the cell appeared to be correlated with the level of kinesin expression. Furthermore, the distribution of the KHC or KHC domains was not influenced by cell size.

The Filamentous Elements That Colocalize with Protein Expressed by pSVKin, pSVTail, and pSVRT Are Cytoplasmic Microtubules

As intermediate filaments often show a similar distribution to microtubules (Hynes and Destree, 1978; Geuens et al., 1983), we examined whether the filamentous staining pattern of the expressed KHC proteins reflects an interaction with intermediate filaments. Fig. 6, *A* and *B*, shows that the rod–tail protein (pSVRT), like the tail domain and the entire KHC, demonstrated a filamentous staining pattern that very closely reflected the microtubule distribution in the transfected cells. When transfected cells were double labeled with antivimentin antibodies, on the other hand, the expressed rod–tail domain colocalizes extensively but not entirely with vimentin intermediate filaments (Fig. 6, *C* and *D*). The lack of colocalization is particularly evident in the periphery, where the vimentin filament network had partially collapsed towards the cell center. This partial collapse was more common in the transfected than the untransfected cells (Fig. 6 *D*), which could be due to the expressed kinesin tail interfering with a kinesin-driven extension of intermediate filaments towards the periphery along microtubules (Gyoeva and Gelfand, 1991).

To further establish that the expressed KHC colocalizes with cytoplasmic microtubules, its distribution was examined after taxol or nocodazole treatment. A brief nocodazole treatment (20 min; 10 μM) was used to depolymerize the majority of the cytoplasmic microtubules (Fig. 7 *A*); this short incubation did not collapse the intermediate filament network. The microtubules that remained intact (many of which were in the perinuclear region) probably correspond to a subset of stable microtubules that have been described in other studies (Schulze and Kirschner, 1987; Kreis, 1987). The expressed KHC (pSVKin) colocalized with the nocoda-

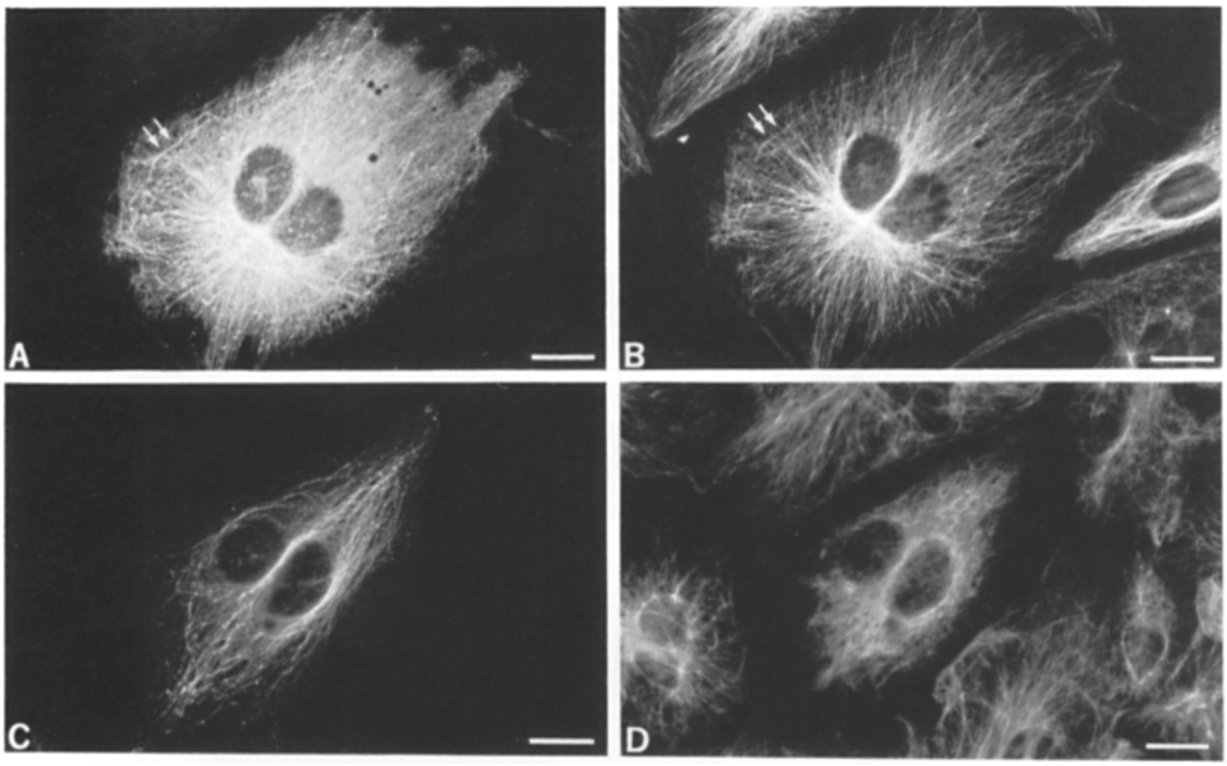

Figure 6. Distributions of microtubules, vimentin filaments, and the expressed kinesin tail (pSVRT) in CV-1 cells. All cells were fixed with methanol–acetone at −20°C and double-labeled with the following primary antibodies: polyclonal IgG against the VSV G protein epitope (*A* and *C*), monoclonal rat IgG against tubulin (*B*), and monoclonal mouse IgG to vimentin (*D*). The pattern of immunofluorescence for the expressed kinesin protein (*A* and *C*) shows a filamentous distribution similar to that of microtubule (*B*), but different from the one of intermediate filaments (*D*). In *A*, a diffuse immunofluorescence is observed throughout the cytoplasm similar to the staining obtained for pSVKin and pSVTail in the same fixation conditions and shown in Fig. 7, *A* and *C*. Such diffuse immunofluorescence is less evident in *C* probably because of a better extraction obtained in these cells with methanol–acetone. Individual filaments decorated by the VSV G peptide antibody appear to coalign with single microtubules (arrows in *A* and *B*), but not with intermediate filaments. Bar, 2 μm.

zole-resistant microtubules surrounding the nucleus (Fig. 7 *A*); the filamentous staining of KHC which normally extends towards the periphery in the transfected cells, (Figs. 5 *A* and 7 *E*) was no longer observed after nocodazole treatment. With a longer nocodazole incubation (1–2 h), neither microtubule nor filamentous KHC staining was evident (not shown). Taxol (20 μM) causes the polymerization of noncentrosomal microtubules, which often become bundled (Fig. 7 *D*) (DeBrabander et al., 1981). In transfected cells treated with taxol, the pSVKin expressed protein colocalized with the taxol-induced microtubule bundles (Fig. 7, *C* and *D*). Similar changes in the distribution of the tail domain expressed from pSVTail were observed after nocodazole and taxol treatment (not shown). The change in distribution of the pSVKin and pSVTail expressed proteins after taxol or nocodazole treatment further supports the notion that these proteins interact with cytoplasmic microtubules or microtubule-associated proteins.

Cells transfected with pSVKin frequently displayed unusual spatial arrangements of cytoplasmic microtubules that were rarely seen in the untransfected cells. In untransfected cells or cells expressing the motor, tail, or the rod–tail domains, microtubules generally emanate from the centrosomal region of the cell and extend towards the periphery (Fig. 5, *D*, *F*, and *H*). In ~50% of the cells expressing the entire KHC, the connection of microtubules to the centrosome was less obvious and the microtubules seemed more disorganized than those in the nontransfected cells (Fig. 7 *E* and *F*).

Discussion

Comparison of Human and Invertebrate KHC Sequences

In this study, we have cloned and characterized the gene encoding the human homologue of the KHC. Comparisons of the human KHC sequence with *Drosophila* (Yang et al., 1989), squid (Kosik et al., 1990), and sea urchin (Wright et al., 1991) KHC sequences reveal a high level of amino acid sequence identity over the entire molecule. The degree of similarity between the invertebrate and mammalian KHCs is particularly striking in the motor domain, where very long stretches of nearly 100% amino acid identity are observed. These domains of high conservation presumably play important roles in ATP hydrolysis, microtubule binding, and force production. The COOH-terminal tail domain also displays extensive segments of nearly complete identity, indicating that it must serve an important, although still unidentified function. This region has been proposed to interact with light chains, organelles, and possibly microtubules. The rod displays significantly less primary sequence homology, except at its COOH-terminal end, which is almost identical in all of the cloned KHCs.

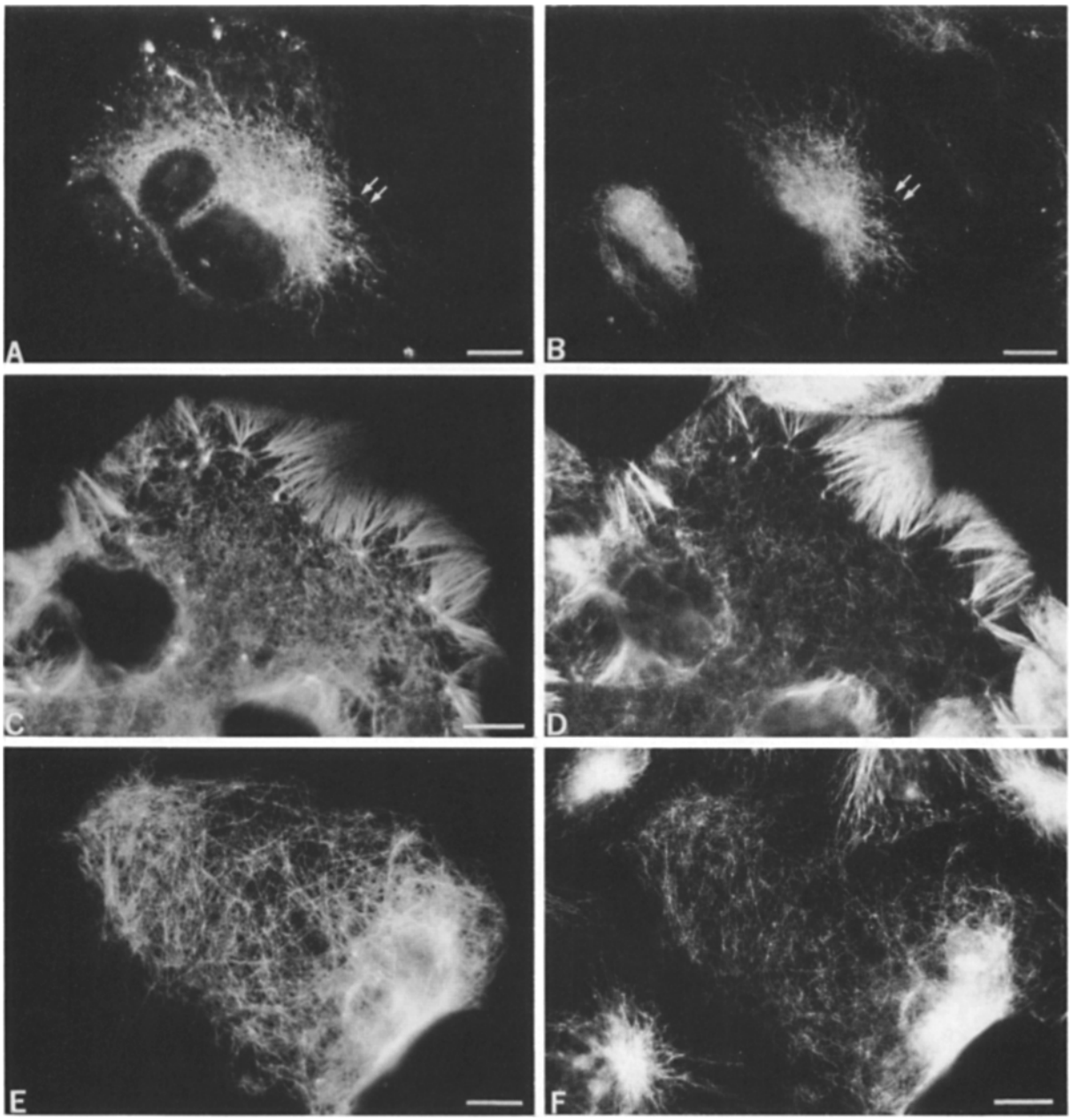

Figure 7. Immunofluorescence localization of the microtubules and the expressed pSVKin after nocodazole or taxol treatment of CV-1 cells transfected with pSVKin. In *A* and *B*, cells were incubated for 6 min in the presence of 10 μM nocodazole; in *C* and *D* they were treated with 20 μM taxol (National Cancer Institute) for 2 h (both at 37°C). Cells in *E* and *F* did not receive any drug treatment. All cells were permeabilized with 0.5% Triton X-100 in 80 mM Pipes, 1 mM EGTA, 1 mM $MgCl_2$ and then fixed in methanol–acetone at −20°C. Cells were double-labeled for the expressed kinesin with the polyclonal anti-VSV G protein epitope antibody (*A*, *C*, and *E*) and for tubulin with the rat monoclonal antibody (*B*, *D*, and *F*). The pattern of distribution of the expressed KHC appears very similar to that of microtubules even when the organization of the microtubular network is modified by nocodazole or taxol treatments. In *A*, filaments decorated with the expressed kinesin coincide with microtubules in *B* that have not yet depolymerized (see arrows for an example). In *C* and *D*, taxol-induced microtubules bundles coincide with localization pattern seen with the anti-VSV G peptide antibody. Cells transfected with pSVKin often show a disorganized microtubule network that does not originate from the centrosomal area (*E* and *F*). The distributions of the expressed kinesin protein and tubulin again appear to coincide. Bars, 2 μm.

We have also found two short stretches (14 and 23 amino acids) of sequence homology between the nonmotor domains of the KHCs and *bimC* (a kinesin-like gene from *Aspergillus* [Enos and Morris, 1990]) that were not noted in previous sequence comparisons. In the 14-amino acid stretch located at the COOH-terminal end of the human KHC rod domain, 10 amino acids are either identical or are similar to those found within a region of the nonmotor domain of *bimC*. In contrast, no sequence homologies were observed between the nonmotor domains of the KHCs and a variety of other kinesin-like motor proteins. Although the regions of sequence similarity between human KHC and *Aspergillus bimC* are relatively small, they nonetheless suggest that the nonmotor domains of these two proteins may have a similar property or function.

We have also identified an upstream ORF and a G-C rich

leader sequence in the 5′ untranslated region of hKHC that may be important for translational regulation. The upstream ORF (nt −226 to −203) contains three tandemly arranged potential start codons which are in the same reading frame; the nucleotides surrounding the first start codon form a perfect consensus sequence for ribosomal initiation of translation (Kozak, 1987). Upstream AUG codons are rare among eukaryotic mRNAs and are not found in the published 5′ untranslated regions of *Drosophila*, squid, and sea urchin kinesins. The ability of upstream ORFs to regulate mRNA translation has been most clearly shown for GCN4, a yeast gene involved in the control of amino acid biosynthesis (for review see Hinnebusch, 1990). In mammalian systems, AUG codons introduced into the 5′-untranslated region of mRNAs can significantly reduce expression of the downstream reading frame (Kozak, 1984; Liu et al., 1984). In addition to the upstream ORF, the human KHC 5′-untranslated region contains regions that are very G-C rich, a characteristic that at least in one case (the c-*sis*/PDGF 2 transcript) has been shown to inhibit translation (Rao et al., 1988). The presence of upstream AUGs and G-C rich regions in the 5′-untranslated region of kinesin mRNA may pose an obstacle to initiation by a ribosome scanning mechanism and could signify internal initiation of translation, as has been documented for mRNAs encoding BiP (Macejak and Sarnow, 1991) and polio virus proteins (Pelletier and Sonnenberg, 1988). Since invertebrate KHC cDNAs have neither upstream ORFs nor the G-C rich leader sequence, it is possible that vertebrates have acquired a means of regulating kinesin expression at the translational level.

Interaction of the Kinesin Motor and Tail Domains with Cytoplasmic Microtubules

Although a good deal is known about the properties of kinesin's motor domain, the functions of the remainder of the molecule are poorly understood. Based upon the overall structure of kinesin (Amos, 1987; Hirokawa et al., 1989; Scholey et al., 1989), the tail is thought to function as an attachment domain, anchoring kinesin to macromolecular structures that are to be transported along microtubules. The fact that the tail domain shows the same degree of amino acid homology as the motor domain amongst kinesins from different species implies a conserved function, possibly that of binding to specific target proteins. One of its binding partners is the kinesin light chain, which has been localized by electron microscopy to the kinesin tail (Hirokawa et al., 1989). However, the tail domain of the KHC may likely interact with other proteins that are important for the biological activities of this motor protein.

In this study, we have found that the KHC and the KHC tail domains expressed in CV-1 cells colocalize with cytoplasmic microtubules but not with vimentin filaments. The distribution patterns of these expressed proteins and of microtubules change in similar ways when cells are treated with taxol or nocodazole, reinforcing the notion that these expressed proteins interact with microtubules and not some other cytoplasmic filamentous network. The expressed KHC proteins containing the tail domain also show a soluble distribution, suggesting possibly that these expressed proteins have a relatively weak affinity for microtubules in a cellular environment.

The expressed motor domain also associates with cytoplasmic microtubules, but only after detergent permeabilization in a nucleotide-free buffer. This treatment most likely produces a rigor-like association between kinesin and the cytoplasmic microtubules. The finding that the motor domain does not localize to microtubules in cells fixed in methanol–acetone or in cells permeabilized with Triton X-100 and MgATP indicates that the expressed motor domain exhibits normal ATP-sensitive microtubule binding. The localization of the tail domain with microtubules, on the other hand, does not seem to be influenced by ATP, suggesting that its interaction with microtubules is not nucleotide sensitive.

An important concern is whether the interaction of the kinesin tail domain with microtubules reflects a specific and biologically meaningful interaction. Microtubule colocalization of the expressed proteins was observed with or without Triton X-100 permeabilization and under two different fixation conditions, indicating that this localization pattern is not a fixation artefact. Furthermore, the expressed kinesin rod domain and the cytoplasmic enzyme β-galactosidase are both randomly distributed throughout the cytoplasm and do not colocalize with microtubules, suggesting at least some specificity of the interaction between the tail domain and microtubules.

The levels of kinesin expression from the vector pose another possible concern. Quantitative video analysis reveals that expression levels vary by more than 100-fold between different cells. Microtubule colocalization, however, is evident in cells expressing low as well as high levels of protein, indicating that it is not a consequence of very high overexpression. The lowest level of kinesin expression in the transfected cells, although fourfold greater than the endogenous kinesin levels, is also not necessarily beyond physiological concentrations. Hollenbeck (1989) has shown that kinesin levels in sympathetic neurons are eightfold greater than those in epidermal fibroblast cells and such levels are probably comparable to those found in some of the transfected cells. Although these levels may be physiological in neurons, one can not rule out the possibility that the different localization patterns of the endogenous and expressed kinesins in CV-1 cells is due to their different expression levels. For example, additional factors (e.g., light chains) could be needed for the proper localization of KHC and their levels may be insufficient to complex with the KHC or KHC tail domain produced by the expression vector. Different localization patterns could also occur if the endogenous and transfected KHCs are products of distinct genes.

Whether the expressed kinesin tail domain is binding to microtubules or indirectly to microtubule-associated proteins is not clear. Several studies with purified kinesin, however, suggest that kinesin's tail domain can bind directly to microtubules. After examining kinesin bound to microtubules with AMP-PNP by electron microscopy, Amos (1987), Hisanaga et al. (1989), and Andrews, B., P. Gallant, B. Schnapp, and T. Reese (personal communication) all suggested that the tail as well as the motor domain can bind to microtubules in vitro. The dark-field scanning transmission electron microscopy study by Andrews et al. clearly shows that single kinesins can crossbridge two microtubules through interactions at opposite ends of the molecule. The *Drosophila* kinesin tail domain produced by in vitro translation did not cosediment with microtubules under the conditions used in these experiments (Yang et al., 1989); however, the bacterially expressed COOH-terminal domain of the sea

urchin KHC recently was found to cosediment with microtubules in an ATP-independent manner (Skoufias, D., and J. Scholey, personal communication). Thus, our observations, taken together with the above in vitro experiments, suggest a microtubule-binding activity of the kinesin COOH-terminal tail domain.

The nonmotor domains of other kinesin-like molecules may also bind to microtubules. This has been demonstrated most convincingly for the NH_2-terminal (nonmotor) domain of KAR3, which when expressed as a β-galactosidase fusion protein in yeast colocalized with cytoplasmic microtubules (Meluh and Rose, 1990). Although the NH_2-terminal domain of KAR3 (aa 1–109) and the COOH-terminal domain of hKHC (890–963) share no sequence similarity, they both contain a large number of basic (His, Arg, Lys: 21% in KAR3 and 25% in hKHC) and proline (8% both in KAR3 and hKHC) residues and relatively few acidic (Asp, Glu: 5.5% both in KAR3 and hKHC) residues; these features are common in other microtubule-binding proteins (Lee et al., 1989; Lewis et al., 1988).

Since kinesin is thought to transport organelles, our expectation was that the expressed KHC or its tail domain would colocalize with cytoplasmic membranes. Several difficulties, however, make it difficult to assess whether any of the expressed KHC is associated with membranes in these experiments. First, a weak membrane association, similar to that of endogenous kinesin, would be difficult to detect amidst the more prominent levels of soluble and microtubule-associated kinesin protein in the transfected cells. Furthermore, an association with small membrane vesicles would be difficult to discern because of the presence of small punctate aggregates of expressed kinesin that arise possibly as an artefact of fixation or overexpression.

Although the results presented in this study do not resolve whether kinesin associates with membranes, the localization of the kinesin and its tail domain to microtubules raises the possibility that kinesin may participate in movements of the microtubule cytoskeleton. The ability of the kinesin COOH-terminal domain to bind to microtubules and the NH_2-terminal domain to bind to and generate movement along microtubules suggests that kinesin could crossbridge and induce sliding between microtubules. In accordance with this notion, purified kinesin causes microtubule–microtubule bending motions in solution (Vale et al., 1985) and has been shown to induce unipolar microtubule asters, presumably by inducing sliding between adjacent microtubules (Urrutia et al., 1991). Furthermore, the disorganization of microtubules in CV-1 cells expressing the intact KHC might somehow arise from microtubule movements generated by a functional motor.

Possible in vivo situations where microtubule sliding may occur include anaphase B type movements in the microtubule overlap zone (Cande and Hogan, 1989) and the sliding of microtubules in neuronal processes (Reinsch et al., 1991). Since kinesin is abundant in neurons, the latter phenomenon represents a particularly intriguing role for a kinesin motor. In their study, Reinsch et al. (1991) show that fluorescently tagged microtubules are transported towards the nerve terminal, the expected direction for slow anterograde transport of the cytoskeleton. Although the mechanism of this transport is unknown, axonal microtubules, whose plus ends are oriented towards the terminal, could be anterogradely transported along a subpopulation of stationary microtubules. Such transport could be mediated by a plus-end motor, such as kinesin, that is anchored onto microtubules via a tail domain and moves along stationary microtubules through a force-generating crossbridge cycle.

Whether or not kinesin participates in microtubule sliding in vivo, however, has not yet been established. We and others (Pfister et al., 1989; Neighbors et al., 1988) have not found an obvious colocalization of endogenous kinesin with cytoplasmic microtubules by immunofluorescence. Although Hollenbeck (1989) documented a colocalization of endogenous kinesin with cytoplasmic microtubules after saponin permeabilization, this pattern may represent an interaction with microtubule-associated membranes rather than with microtubules themselves. Thus, if kinesin crossbridges microtubules and induces microtubule sliding in cells, the immunolocalization data suggest that it must either be driven by a subset of the kinesin motors or must be regulated so as to occur only under certain circumstances. Thus, further work is required to establish whether the microtubule binding activity of the tail domain actually is manifested under physiological conditions.

We are indebted to Jon Kull for his assistance in the secondary structure predictions, Dr. G. Fungalli for assistance with quantitative analysis of the fluorescence images, and Dr. V. Sheffield for assistance with PCR. We also thank Drs. K. Kosik and L. Goldstein for sharing kinesin sequence information before publication; Drs. T. Kreis, R. Duden, and J. Kilmartin for antibodies; the National Cancer Institute for their gift of taxol; and P. Tinelli for photographic assistance. F. Navone is also grateful to Drs. A. Zanini and N. Borgese for encouragement and discussion.

This work was supported by a National Institutes of Health grant (GM38499) and fellowships from the Klingenstein and Rita Allen Foundations.

Received for publication 27 November 1991 and in revised form 13 March 1992.

References

Amos, L. A. 1987. Kinesin from pig brain studied by electron microscopy. *J. Cell Sci.* 87:105–111.

Bloom, G. S., M. C. Wagner, K. K. Pfister, and S. T. Brady. 1988. Native structure and physical properties of bovine brain kinesin and identification of the ATP-binding subunit polypeptide. *Biochemistry.* 27:3409–3416.

Brady, S. T., K. K. Pfister, and G. S. Bloom. 1990. A monoclonal antibody against kinesin inhibits both anterograde and retrograde fast axonal transport in squid axoplasm. *Proc. Natl. Acad. Sci. USA.* 87:1061–1065.

Cande, W. Z., and C. J. Hogan. 1989. The mechanism of anaphase spindle elongation. *Bioessays.* 11:5–9.

DeBrabander, M., G. Geuens, R. Nuydens, R. Willebrords, and J. DeMey. 1981. Taxol induces the assembly of free microtubules in living cells and blocks the organizing capacity of centrosomes and kinetochores. *Proc. Natl. Acad. Sci. USA.* 78:5608–5611.

de Cuevas, M., T. Tao, and L. S. B. Goldstein. 1992. Evidence that the stalk of Drosophila kinesin heavy chain is an α-helical coiled coil. *J. Cell Biol.* 116:957–965.

Endow, S. A. 1991. The emerging kinesin family of microtubule motor proteins. *Trends. Biochem. Sci.* 16:221–225.

Endow, S. A., S. Henikoff, and L. Soler-Niedziela. 1990. Mediation of meiotic and early mitotic chromosome segregation in Drosophila by a protein related to kinesin. *Nature (Lond.).* 345:81–83.

Enos, A. P., and N. R. Morris. 1990. Mutation of a gene that encodes a kinesin-like protein blocks nuclear division in *A. nidulans*. *Cell.* 60:1019–1027.

Ferreira, A., J. Niclas, R. D. Vale, G. Banker, and K. S. Kosik. 1992. Suppression of kinesin expression in cultured hippocampal neurons using antisense oligonucleotides. *J. Cell Biol.* In press.

Finer-Moore, J., and R. M. Stroud. 1984. Amphiphatic analysis and possible formation of the ion channel in an acetylcholine receptor. *Proc. Natl. Acad. Sci. USA.* 81:155–159.

Friederich, E., C. Huet, M. Arpin, and D. Louvard. 1989. Villin induces microvilli growth and actin redistribution in transfected fibroblasts. *Cell.* 59: 461–475.

Geuens, G., M. DeBrabander, R. Nuydens, and J. DeMey. 1983. The interac-

tion between microtubules and intermediate filaments in cultured cell treated with taxol and nocodazole. *Cell Biol. Int. Rep.* 7:35–47.
Goldstein, L. S. B. 1991. The kinesin superfamily: tails of redundancy. *Trends Cell Biol.* 1:93–98.
Gyoeva, F. K., and V. I. Gelfand. 1991. Coalignment of vimentin intermediate filaments with microtubules depends on kinesin. *Nature (Lond.).* 353:445–448.
Hagan, I., and M. Yanagida. 1990. Novel potential mitotic motor protein encoded by the fission yeast cut7+ gene. *Nature (Lond.).* 347:563–566.
Henikoff, S. 1987. Unidirectional digestion with exonuclease III in DNA sequence analysis. *Methods Enzymol.* 155:156–165.
Hinnebusch, A. G. 1990. Involvement of an initiation factor and protein phosphorylation in translational control of GCN4 mRNA. *Trends Biol. Sci.* 15: 148–152.
Hirokawa, N., K. K. Pfister, H. Yorifuji, M. C. Wagner, S. T. Brady, and G. S. Bloom. 1989. Submolecular domains of bovine brain kinesin identified by electron microscopy and monoclonal antibody decoration. *Cell.* 56: 867–878.
Hirokawa, N., R. Sato-Yoshitake, N. Kobayashi, K. K. Pfister, G. S. Bloom, and S. T. Brady. 1991. Kinesin associates with anterogradely transported membranous organelles. *J. Cell Biol.* 114:295–302.
Hisanaga, S., H. Murofushi, S. Okuhara, R. Sato, Y. Masuda, H. Sakai, and N. Hirokawa. 1989. The molecular structure of adrenal medulla kinesin. *Cell Motil. Cytoskeleton.* 16:264–272.
Hollenbeck, P. J. 1989. The distribution, abundance and subcellular localization of kinesin. *J. Cell Biol.* 108:2335–2342.
Hollenbeck, P. J., and J. A. Swanson. 1990. Radial extension of macrophage tubular lysosomes supported by kinesin. *Nature (Lond.).* 346:864–866.
Huylebroeck, D., G. Maertens, M. Verhoeyen, C. Lopez, A. Raeymakers, W. M. Jou, and W. Fiers. 1988. High-level transient expression of influenza virus proteins from a series of SV 40 late and early replacement vectors. *Gene (Amst.).* 66:163–181.
Hynes, R. O., and A. T. Destree. 1978. 10 nm filaments in normal and transformed cells. *Cell.* 13:151–163.
Kosik, K. S., L. D. Orecchio, B. Schnapp, H. Inouye, and R. L. Neve. 1990. The primary structure and analysis of the squid kinesin heavy chain. *J. Biol. Chem.* 265:3278–3283.
Kozak, M. 1984. Selection of initiation sites by eucaryotic ribosomes: effect of inserting AUG triplets upstream from the coding sequence for preproinsulin. *Nucleic Acids Res.* 12:3873–3893.
Kozak, M. 1987. An analysis of 5'-noncoding sequences from 699 vertebrate messenger RNAs. *Nucleic Acids Res.* 15:8125–8148.
Kreis, T. E. 1986. Microinjected antibodies against the cytoplasmic domain of vesicular stomatitis virus glycoprotein block its transport to the cell surface. *EMBO (Eur. Mol. Biol. Organ.) J.* 5:931–941.
Kreis, T. E. 1987. Microtubules containing detyrosinated tubulin are less dynamic. *EMBO (Eur. Mol. Biol. Organ.) J.* 6:2597–2606.
Kuznetsov, S. A., E. A. Vaisberg, N. A. Shanina, N. N. Magretova, V. Y. Chernyak, and V. I. Gelfand. 1988. The quarternary structure of bovine brain kinesin. *EMBO (Eur. Mol. Biol. Organ.) J.* 7:353–356.
Kuzenetsov, S. A., Y. A. Vaisberg, S. W. Rothwell, D. B. Murphy, and V. I. Gelfand. 1989. Isolation of a 45-kDa fragment from the kinesin heavy chain with enhanced ATPase and microtubule-binding activity. *J. Biol. Chem.* 264: 589–595.
Laemmli, U. 1970. Cleavage of structural proteins during assembly of the bacteriophage T4. *Nature (Lond.).* 227:680–685.
Lawrence, C. B., and D. A. Goldman. 1988. Definition and identification of homology domains. *Compot. Appl. Biosci.* 4:25–31.
Lee, G., R. L. Neve, and K. S. Kosik. 1989. The microtubule binding domain of tau. *Neuron.* 2:1615–1624.
Lewis, S. A., D. Wang, and N. J. Cowan. 1988. Microtubule-associated protein MAP2 shares a microtubule binding motif with tau protein. *Science (Wash. DC).* 242:936–939.
Liu, C.-C., C. C. Simonsen, and A. D. Levinson. 1984. Initiation of translation at internal AUG codons in mammalian cells. *Nature (Lond.).* 309:82–85.
Macejak, D. G., and P. Sarnow. 1991. Internal initiation of translation mediated by the 5' leader of a cellular mRNA. *Nature (Lond.).* 353:90–93.
Maniatis, T., E. F. Fritsch, and J. Sambrook. 1982. Molecular Cloning: A laboratory manual. Cold Spring Harbor Laboratory, Cold Spring Harbor, NY. 545 pp.
Maxam, A. M., and W. Gilbert. 1977. A new method for sequencing DNA. *Proc. Natl. Acad. Sci. USA.* 74:560–564.
McDonald, H. B., and L. S. B. Goldstein. 1990. Identification and characterization of a gene encoding a kinesin-like protein in Drosophila. *Cell.* 61:991–1000.
Meluh, P. M., and M. D. Rose. 1990. KAR3, a kinesin-related gene required for yeast nuclear fusion. *Cell.* 60:1029–1041.
Mullis, K., F. Faloona, S. Scharf, R. Saiki, G. Horn, and H. Erlich. 1986. Specific enzymatic amplification of DNA in vitro: the polymerase chain reaction. *Cold Spring Harbor Symp. Quant. Biol.* LI:263–273.
Neighbors, B. W., R. C. Williams, Jr., and J. R. McIntosh. 1988. Localization of kinesin in cultured cells. *J. Cell Biol.* 106:1193–1204.
Olmsted, J. B. 1981. Affinity purification of antibodies from diazotized paper blots of heterogenous protein samples. *J. Biol. Chem.* 256:11955–11957.
Otsuka, A. J., A. Jeyaprakash, J. Garcia-Anoveros, L. Z. Tang, G. Fisk, T. Hartshorne, R. Franco, and T. Born. 1991. The *C. elegans* unc-104 gene encodes a putative kinesin heavy chain-like protein. *Neuron.* 6:113–122.
Pelletier, J., and N. Sonnenberg. 1988. Internal initiation of translation of eukaryotic mRNA directed by a sequence derived from poliovirus RNA. *Nature (Lond.).* 334:320–325.
Pfister, K. K., M. C. Wagner, D. L. Stenoien, S. T. Brady, and G. S. Bloom. 1989. Monoclonal antibodies to kinesin heavy and light chains stain vesicle-like structures, but not microtubules, in cultured cells. *J. Cell Biol.* 108: 1453–1464.
Rao, C. D., M. Pech, K. C. Robbins, and S. A. Aaronson. 1988. The 5' untranslated sequence of the c-sis/platelet-derived growth factor 2 transcript is a potent translational inhibitor. *Mol. Cell. Biol.* 8:284–292.
Reinsch, S. S., T. J. Mitchison, and M. Kirschner. 1991. Microtubule polymer assembly and transport during axonal elongation. *J. Cell Biol.* 115:365–379.
Rodionov, V. L., F. K. Gyoeva, and V. I. Gelfand. 1991. Kinesin is responsible for centrifugal movement of pigment granules in melanophores. *Proc. Natl. Acad. Sci. USA.* 88:4956–4960.
Sanger, F., S. Nicklen, and A. Coulson. 1977. DNA sequencing with chain terminating inhibitors. *Proc. Natl. Acad. Sci. USA.* 74:5463–5467.
Saxton, W. M., J. Hicks, L. S. B. Goldstein, and E. C. Raff. 1991. Kinesin heavy chain is essential for viability and neuromuscular functions in Drosophila, but mutants show no defects in mitosis. *Cell.* 64:1093–1102.
Scholey, J. M., J. Heuser, J. T. Yang, and L. S. B. Goldstein. 1989. Identification of globular mechanochemical heads of kinesin. *Nature (Lond.).* 338: 355–357.
Schulze, E., and M. Kirschner. 1987. Dynamic and stable populations of microtubules in cells. *J. Cell Biol.* 104:277–288.
Towbin, H., T. Staehelin, and J. Gordon. 1979. Electrophoretic transfer of proteins from polyacrylamide gels to nitrocellulose sheets: procedure and some applications. *Proc. Natl. Acad. Sci. USA.* 76:4350–4354.
Urrutia, R., M. A. McNiven, J. P. Albanesi, D. B. Murphy, and B. Kachar. 1991. Purified kinesin promotes vesicle motility and induces active sliding between microtubules *in vitro*. *Proc. Natl. Acad. Sci. USA.* 88:6701–6705.
Vale, R. D. 1987. Intracellular transport using microtubule-based motors. *Annu. Rev. Cell Biol.* 3:347–378.
Vale, R. D., and L. S. B. Goldstein. 1990. One motor, many tails: an expanding repertoire of force-generating enzymes. *Cell.* 60:883–885.
Vale, R. D., B J. Schnapp, T. Mitchison, E. Steuer, T. S. Reese, and M. P. Sheetz. 1985. Different axoplasmic proteins generate movement in opposite directions along microtubules in vitro. *Cell.* 43:623–632.
Wright, B. D., J. H. Henson, K. P. Wedaman, P. J. Willy, J. N. Morand, and J. M. Scholey. 1991. Subcellular localization and sequence of sea urchin kinesin heavy chain: evidence for its association with membranes in the mitotic apparatus and interphase cytoplasm. *J. Cell Biol.* 113:817–833.
Yang, J. T., R. A. Laymon, and L. S. B. Goldstein. 1989. A three-domain structure of kinesin heavy chain revealed by DNA sequence and microtubule binding analyses. *Cell.* 56:879–889.
Yang, J. T., W. M. Saxton, R. J. Stewart, E. C. Raff, and L. S. Goldstein. 1990. Evidence that the head of kinesin is sufficient for force generation and motility in vitro. *Science (Wash. DC).* 249:42–47.
Zhang, P., B. A. Knowles, L. S. B. Goldstein, and R. S. Hawley. 1990. A kinesin-like protein required for distributive chromosome segregation in Drosophila. *Cell.* 62:1053–1062.